J. Phys. B: At. Mol. Opt. Phys. **33** (2000) 3293–3305. Printed in the UK PII: S0953-4075(00)50358-7

Elastic and total cross sections for electron–carbonyl sulfide collisions

S E Michelin†, T Kroin†, I Iga‡, M G P Homem§, H S Miglio‡ and M T Lee‡

† Departamento de Física, Universidade Federal de Santa Catarina, 88049, Florianópolis, SC, Brazil

‡ Departamento de Química, Universidade Federal de São Carlos, 13565-905, São Carlos, SP, Brazil

§ Departamento de Física, Universidade Federal de São Carlos, 13565-905, São Carlos, SP, Brazil

Received 22 March 2000, in final form 8 June 2000

Abstract. In this paper, we report a joint theoretical–experimental study on electron–OCS collisions in the low- and intermediate-energy ranges. More specifically, elastic differential and integral cross sections, as well as grand total (elastic + inelastic) cross sections in the 0.4–600 eV energy range, are reported. A complex optical potential consisting of static, exchange, correlation–polarization plus absorption contributions, derived from a fully molecular wavefunction, is used for the electron–molecule interaction. The Schwinger variational iterative method, combined with the distorted-wave approximation, is applied to calculate the scattering amplitudes. Additionally, we also report measured elastic differential and integral cross sections in the 100–600 eV energy range determined using the relative-flow technique. Comparison between calculated results and present and existing experimental data, as well as with other theoretical results, is encouraging.

1. Introduction

Among triatomic linear molecules, CO_2, OCS and CS_2 form a very important group due to numerous applications in astrophysics and atmospheric studies. From a scientific point of view, this group is interesting as well. The three molecules are isoelectronic in the valence shell. Although the similarity between their electronic ground-state configurations may lead to similarities in the electron impact spectra, the sulfur atom in OCS and CS_2 with low-lying d orbitals can influence both the chemical bonding (Hehere *et al* 1986), and the ionization dynamics. Unlike CO_2 and CS_2, OCS has a permanent dipole moment (0.712 D). This aspect certainly influences the collisional dynamics with charged particles such as electrons, positrons and protons. For example, the direct-scattering mechanism proceeds dominantly via the dipole potential for elastic electron–polar molecule collisions in the low impact energy range. Because of its moderate dipole moment, investigations on e^-–OCS scattering link similar studies on weak and strong polar molecules (Sohn *et al* 1987).

Despite that, electron scattering by OCS has attracted relatively little attention during the past decades. On the experimental aspect, some early investigations reported in the literature include those of Tronc *et al* (1979) and Abouaf *et al* (1994) for the elastic and vibrational electron scattering in the low-energy range and Ziesel *et al* (1980) for the dissociative attachment studies. Total (elastic + inelastic) cross sections (TCS) for e^-–OCS scattering were reported by Szmytkowski *et al* (1984, 1989), Dababneh *et al* (1985) and Zecca *et al* (1995). Very recently, total and elastic integral cross sections for electron and positron scattering from

0953-4075/00/173293+13$30.00

OCS were also investigated by Sueoka *et al* (1999). On the other hand, very few studies have been done on the experimental determination of absolute differential cross sections (DCS) for elastic electron–OCS collisions. To our knowledge, only two such measurements have been carried out. Sohn *et al* (1987) have reported DCS for vibrationally elastic and inelastic e^-–OCS collisions in the 0.4–5.0 eV range. Very recently, absolute DCS for elastic electron scattering on this molecule over a wide energy range (1.5–100 eV) were also measured by Tanaka (2000). For incident energies above 100 eV, there are no reported experimental DCS.

On the theoretical side, the literature for e^-–OCS scattering is even more scarce. A comparative study for low-energy electron scattering by CO_2, OCS, and CS_2 was carried out using the continuum multiple-scattering method (CMSM) (Lynch *et al* 1979). In their calculated integral elastic cross sections (ICS) a sharp resonance at incident energy below 4 eV was predicted for all these molecules. Such resonance structures were observed as well in the experiments (Sohn *et al* 1987, Szmytkowski *et al* 1984) for CO_2 and OCS. However these were not seen in the electron–CS_2 interaction. Very recently, we have reported a theoretical investigation on the elastic e^-–CS_2 scattering in the 1–100 eV range (Lee *et al* 1999). In that study, a complex optical potential derived from a fully molecular near-Hartree–Fock SCF wavefunction was applied to describe the electron–molecule interaction. The Lippmann–Schwinger scattering equations were solved using the Schwinger variational iterative method (SVIM) (Lucchese *et al* 1982, Lee *et al* 1992) combined with the distorted-wave approximation (DWA) (Fliflet and McKoy 1980, Lee and McKoy 1983, Lee *et al* 1990a, Michelin *et al* 1996). Our study showed no evidence of resonances in the 1–4 eV range for elastic e^-–CS_2 scattering, which is in accordance with the experimental observations (Sohn *et al* 1987, Szmytkowski 1987). Since OCS is intermediate between CO_2 and CS_2 in molecular size, the verification of this shape resonance by theoretical calculation will be interesting.

In the present paper, we report a joint theoretical and experimental study on electron scattering by OCS in the low- and intermediate-energy ranges. More especially, calculated TCS and elastic DCS and ICS for electron impact energies up to 600 eV, as well as measured DCS and ICS in the 100–600 eV range, are reported. The calculation scheme is the same as used in our recent studies for CO_2 (Iga *et al* 1999), CS_2 (Lee *et al* 1999), and CH_4 (Iga *et al* 2000). On the other hand, the relative-flow method is applied on the determination of absolute DCS and ICS.

The organization of this paper is as follows: in section 2, we describe briefly the theory used and also give some details of the calculation. In section 3 some details of the measurements are presented and finally in section 4 we compare our calculated results with the present measured data and with some other experimental and theoretical data available in the literature.

2. Theory and calculation

Since the details of the SVIM (Lucchese *et al* 1982) and the DWA (Fliflet and McKoy 1980, Lee and McKoy 1983, Lee *et al* 1990a) have already been presented in our previous papers, here we will only outline briefly the theory used. Within the fixed-nuclear framework, the electron–molecule scattering dynamics is represented by a complex optical potential, given by

$$V_{\mathrm{opt}}(\vec{r}) = V^{\mathrm{SEP}}(\vec{r}) + \mathrm{i}V_{ab}(\vec{r}) \tag{1}$$

where the V^{SEP} is the real part of the interaction potential formed by the static, the exchange and the correlation–polarization contributions whereas V_{ab} is the absorption potential. In our calculation, V_{st} and V_{ex} are derived exactly from an SCF target wavefunction, while V_{cp} is obtained in the framework of the free-electron-gas (FEG) model derived from a parameter-free local density, as prescribed by Padial and Norcross (1984). The dipole polarizabilities

$\alpha_0 = 37.38$ au and $\alpha_2 = 27.20$ au (Hirschfelder *et al* 1954) were used to calculate the asymptotic form of V_{cp}. Further, the quasi-free scattering model, version 3, of Staszewska *et al* (1984) is used for the absorption potential.

Next, the Lippmann–Schwinger scattering equation for elastic electron–OCS collisions is solved using the SVIM with the real part of the optical potential. In the SVIM calculations, the continuum wavefuntions are single-centre expanded as

$$\chi_{\vec{k}}(\vec{r}) = (2/\pi)^{1/2} \sum_{lm} \frac{(\mathrm{i})^l}{k} \chi_{klm}(\vec{r}) Y_{lm}(\hat{k}), \tag{2}$$

where $Y_{lm}(\hat{k})$ are the usual spherical harmonics. The absorption part of the T matrix is calculated via the DWA as

$$T_{ab} = \mathrm{i}\langle \chi_f^- | V_{ab} | \chi_i^+ \rangle. \tag{3}$$

The electronic configuration of the ground-state OCS is $1\sigma^2 2\sigma^2 3\sigma^2 4\sigma^2 5\sigma^2 1\pi^4 6\sigma^2 7\sigma^2 8\sigma^2 9\sigma^2 2\pi^4 3\pi^4$, $\mathrm{X}\,^1\Sigma^+$. In the SCF calculation, the basis sets used for carbon and oxygen are the standard [10s6p/5s3p] type (Dunning 1971) augmented by three s ($\alpha = 0.0453, 0.0157$, and 0.0051), two p ($\alpha = 0.032\,37$ and 0.931), and two d ($\alpha = 1.373$ and 0.433) uncontracted functions for a carbon atom and by two s ($\alpha = 0.0433, 0.015$), two p ($\alpha = 0.091\,16$ and $0.032\,32$), and two d ($\alpha = 1.433$ and 0.311) uncontracted functions for oxygen. For the sulfur centre, a standard [9s5p/6s4p] basis set (Huzinaga 1965) augmented by two s ($\alpha = 0.0459$ and 0.0171), two p ($\alpha = 0.0502$ and 0.0173), and two d ($\alpha = 1.533$ and 0.344) uncontracted functions is used. With this basis set, the calculated SCF energy and dipole moment, at the experimental equilibrium geometry of the ground-state OCS ($R_{\mathrm{O-C}} = 2.1868$ au and $R_{\mathrm{C-S}} = 2.9491$ au), are -510.2988 and $0.310\,56$ au. This result compares well with previously calculated SCF values of -510.2967 and 0.310 au (Bündgen *et al* 1995). The experimental permanent dipole moment is 0.2833 au.

In the present study, we have limited the partial-wave expansions for the continuum wavefunctions as well as for the T-matrix elements up to $l_{\max} = 45$ and $m_{\max} = 15$. Further contributions from the higher partial waves to DCS were accounted for via the Born-closure procedure (Lee *et al* 1990b). On the other hand, it is well known that ICS for electron–polar molecule scattering calculated using the fixed-nuclei approximation diverge at all incident energies due to the divergent DCS in the forward direction. This divergence can be removed only by the introduction of the nuclear motion in the Hamiltonian. Nevertheless, in order to avoid such divergent behaviour, we have calculated the ICS using only the truncated T-matrix elements obtained by SVIM according to the formula

$$\sigma = \frac{4\pi}{k^2} \sum_{ll'm} |T^{\mathrm{SVIM}}_{k,ll'm}|^2. \tag{4}$$

Finally, the total cross sections (TCS) for electron–molecule scattering are also obtained with the truncated T-matrix elements using the optical theorem.

3. Experimental

Details of our experimental set-up and procedure have already been presented elsewhere (Iga *et al* 1999, 2000). Basically, a crossed electron-beam–molecular-beam technique is applied to measure the relative intensity of the scattered electrons as a function of scattering angles.

The electron gun used is of simple design composed of a hairpin tungsten filament, a triode extraction, a set of einzel lenses, and two sets of electrostatic deflectors which allow better positioning of the electron beam in the interaction region. The electron beam is generated

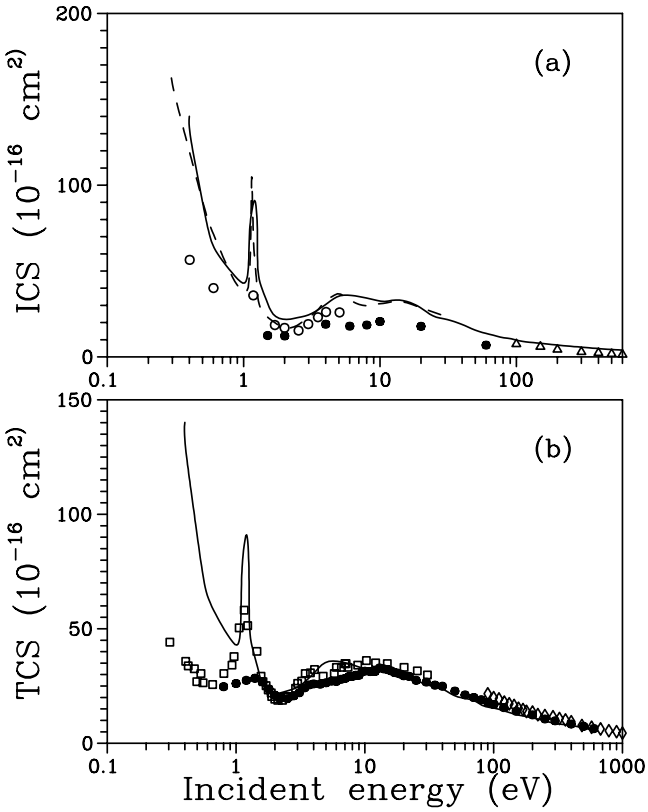

Figure 1. (*a*) Elastic ICS and (*b*) TCS for e^-–OCS scattering in the 0.4–600 eV energy range. Solid curve, present calculated results; dashed curve, calculated results of Lynch *et al* (1979); open circles, experimental data of Sohn *et al* (1987); full circles, experimental data of Sueoka *et al* (1999); open triangles, present measured data; open squares, experimental data of Szmytkowski *et al* (1984, 1989); open diamonds, experimental data of Zecca *et al* (1995).

without prior energy selection. A typical beam current of hundreds of nA is obtained in the covered energy range, with an estimated diameter of 1 mm. A molecular beam flows into the vacuum chamber via a capillary array. This array has an external diameter 1 mm with individual capillaries of diameter (D) 0.05 mm and length (L) 5 mm (aspect ratio $\gamma = D/L = 0.01$). The scattered electrons are energy filtered by a retarding-field energy selector (RFES). The resolution of the RFES is about 1.5 eV for an incident energy of 500 eV. With this resolution, it is sufficient to distinguish inelastically scattered electrons resulting from electronic excitation for the molecule under study since the lowest excitation threshold of OCS is 4.95 eV (Sohn *et al* 1987). Nevertheless, it is unable to separate those from vibrational excitation processes. After energy analysis, the elastically scattered electrons are detected by a channeltron.

During the measurements, the working pressure in the vacuum chamber is around 5×10^{-7} Torr. The recorded scattering intensities are converted into absolute elastic DCS using the relative flow technique (RFT) (Srivastava *et al* 1975, Brinkman and Trajmar 1981, Khakoo and Trajmar 1986, Nickel *et al* 1989, Brunger *et al* 1991, Alle *et al* 1992, Buckman *et al* 1993, Khakoo *et al* 1993, Tanaka *et al* 1998). Accordingly, the DCS for a gas under

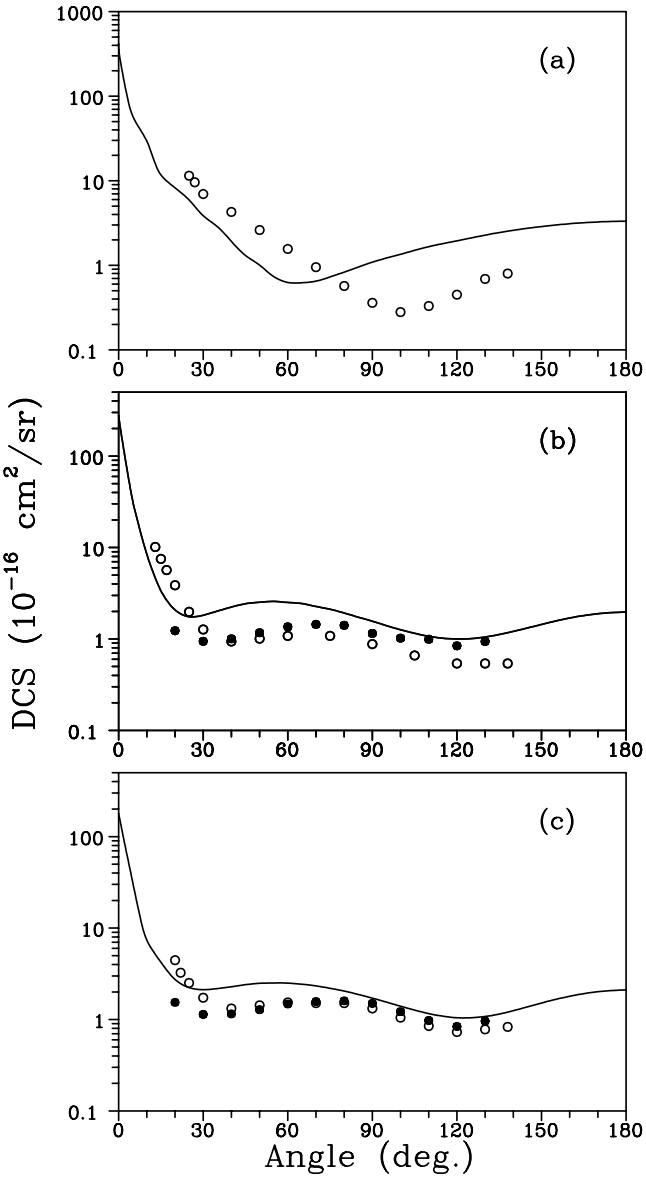

Figure 2. DCS for elastic e^-–OCS scattering at (*a*) 1.15 eV, (*b*) 2 eV, and (*c*) 3 eV. Solid curve, present calculated results; open circles, experimental data of Sohn *et al* (1989); full circles, experimental data of Tanaka *et al* (1999).

determination, x, can be related to the known DCS of a secondary standard, std, as

$$(\mathrm{DCS})_x = (\mathrm{DCS})_{\mathrm{std}} \frac{I_x}{I_{\mathrm{std}}} \frac{n_{\mathrm{std}}}{n_x} \left(\frac{M_{\mathrm{std}}}{M_x} \right)^{\frac{1}{2}}, \tag{5}$$

where I is the scattered electron intensity, n is the flow rate and M is the molecular weight. The above equation is valid if the beam profiles (density distribution) of both gases, x and std, are almost the same. According to Olander and Kruger (1970), this requirement is fulfilled

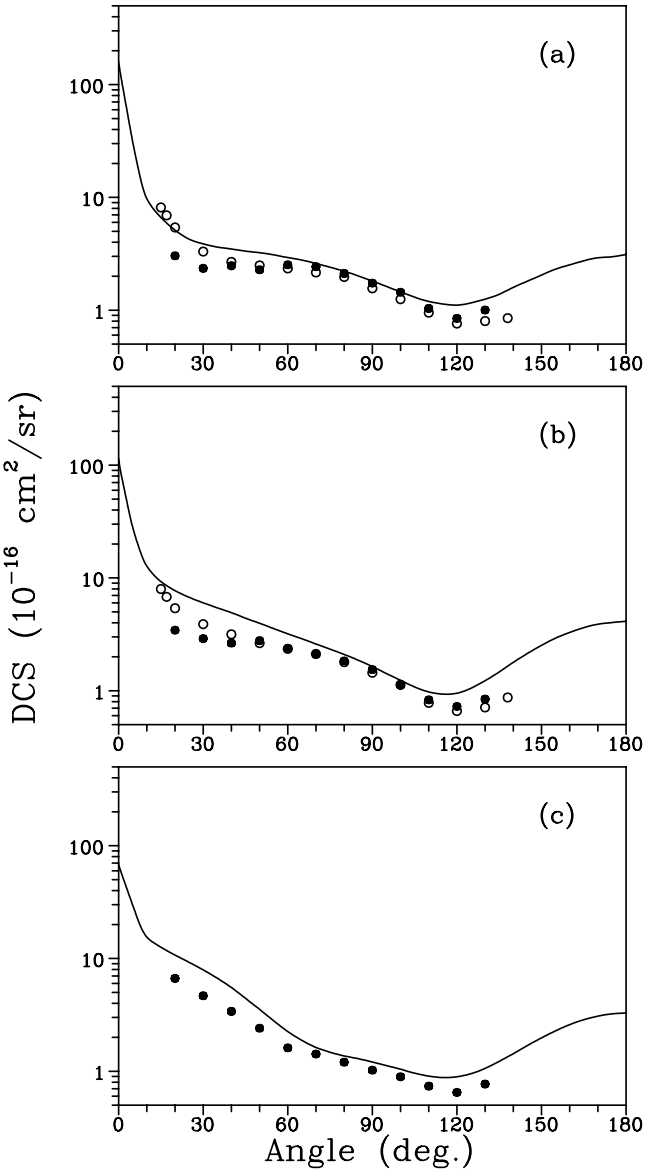

Figure 3. DCS for elastic e^-–OCS scattering at (*a*) 4 eV, (*b*) 5 eV, and (*c*) 8 eV. Solid curve, present calculated results; open circles, experimental data of Sohn *et al* (1989); full circles, experimental data of Tanaka *et al* (1999).

under two conditions: the equal mean free paths (λ) of the gases behind the capillaries and the Knudsen number K_L, defined as $\frac{\lambda}{L}$, varying between $\gamma \leqslant K_L \leqslant 10$. However, several recent investigations have provided experimental evidence that, even at beam flow regimes in which the K_L are significantly lower than γ, the above relationship can still be valid (Buckman *et al* 1993, Tanaka *et al* 1998).

In the present paper, Ar are used as the reference gas. The collisional diameters of Ar and OCS are 2.95 (Roth 1982) and 3.59 Å, respectively. The latter was calculated using the van

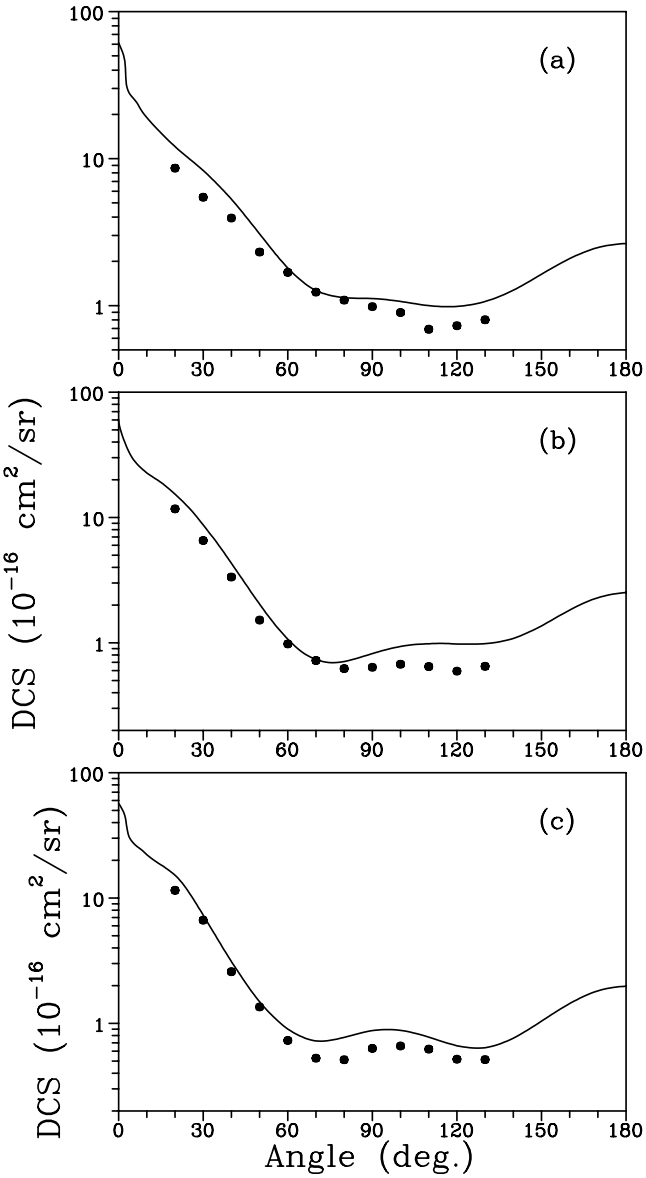

Figure 4. DCS for elastic e^-–OCS scattering at (*a*) 10 eV, (*b*) 15 eV, and (*c*) 20 eV. Solid curve, present calculated results; full circles, experimental data of Tanaka *et al* (1999).

der Waals' constants published in the *Handbook of Chemistry and Physics* (Lide 1993). Thus the theoretical pressure ratio for equal Knudsen numbers will be 1.5 : 1. We used 5.2 Torr for Ar and 3.5 Torr for OCS. This corresponds to a mean free path of 15.5 μm and $K_L = 0.0031$ for both gases. In addition, the absolute cross sections of Jansen *et al* (1976) for Ar are used for the normalization of our data.

Details of the analysis on experimental uncertainties have also been given elsewhere (Iga *et al* 1999, 2000). Briefly, they are estimated as follows. Uncertainties of a random nature, such as the pressure fluctuations, electron beam current readings, the background scattering, etc,

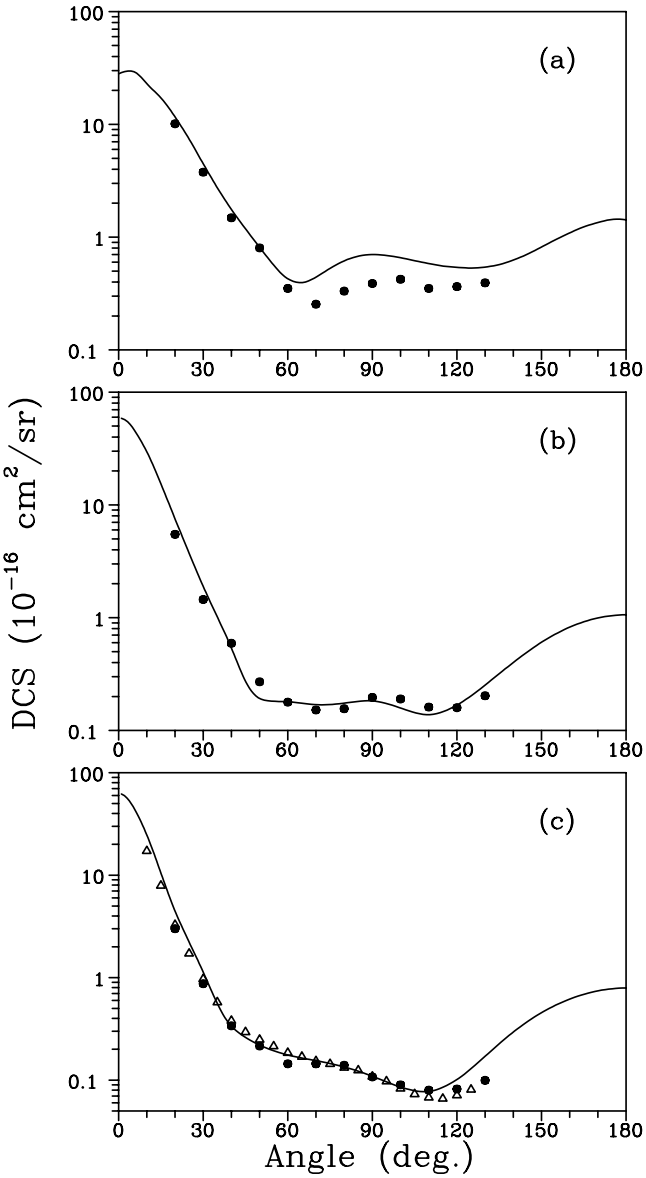

Figure 5. DCS for elastic e^-–OCS scattering at (*a*) 30 eV, (*b*) 60 eV, and (*c*) 100 eV. Solid curve, present calculated results; full circles, experimental data of Tanaka *et al* (1999); open triangles, present experimental DCS.

are estimated to be less than 2%. These contributions, combined with the estimated statistical errors, give an overall uncertainty of 4% on the relative DCS for each gas. Moreover, the quoted errors on the absolute DCS of Jansen *et al* (1976) is 6.5%. In addition, the experimental uncertainty associated with the normalization procedure is estimated to be 5.7%. Therefore, the overall experimental uncertainty on our absolute DCS is about 11%.

In order to obtain the ICS, DCS of the limited angular range have to be extrapolated both at low and high values of angles. A manual extrapolation procedure was carried out which led to estimated overall errors of 20% in ICS.

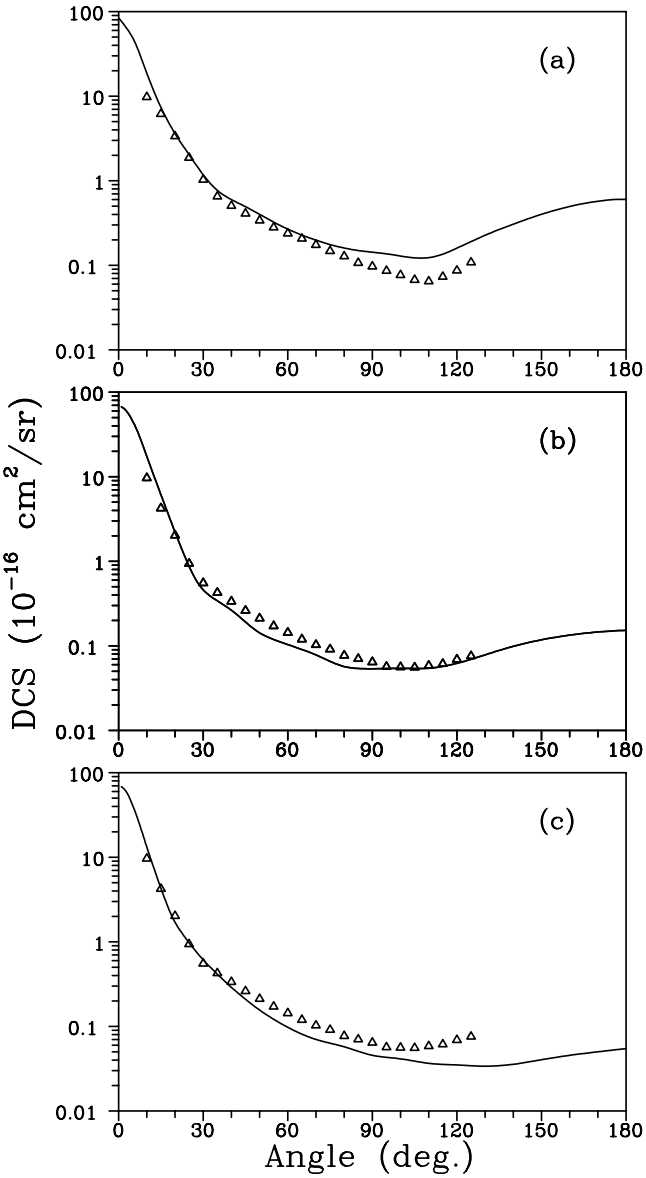

Figure 6. DCS for elastic e^-–OCS scattering at (*a*) 150 eV, (*b*) 200 eV, and (*c*) 300 eV. Solid curve, present calculated results; open triangles, present experimental DCS.

4. Results and discussion

In figures 1(*a*) and (*b*) we show our calculated elastic ICS and TCS in the 0.4–600 eV range, respectively, along with the present measured ICS in the 100–600 incident energy range. Some experimental results of ICS (Sohn *et al* 1987, Sueoka *et al* 1999) and TCS (Szmytkowski *et al* 1984, 1989, Sueoka *et al* 1999) reported in the literature, as well as the calculated ICS of Lynch *et al* (1979) using the CMSM, are also shown for comparison. The measured TCS of Dababneh *et al* (1985) are essentially the same as Sueoka *et al* (1999) and are not shown to

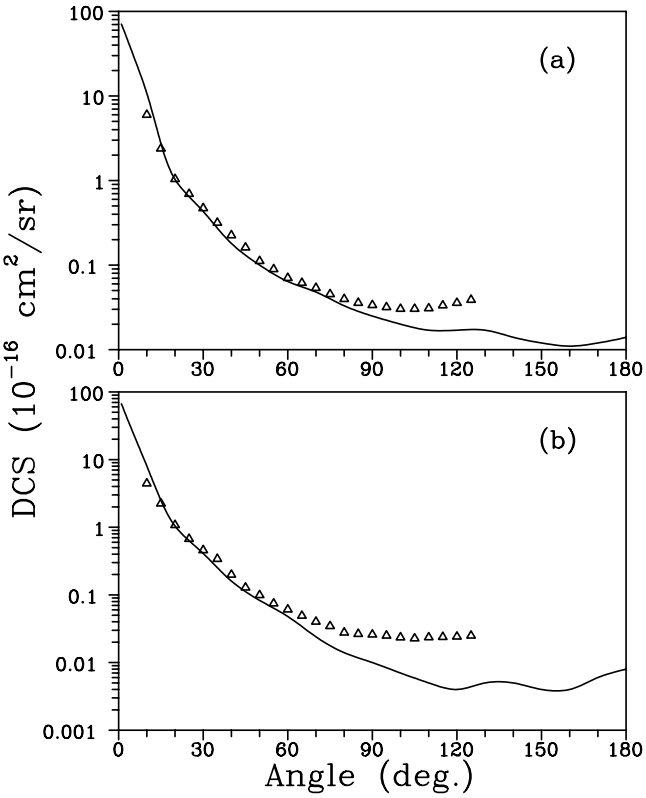

Figure 7. DCS for elastic e^-–OCS scattering at (*a*) 400 eV and (*b*) 600 eV. Solid curve, present calculated results; open triangles, present experimental DCS.

avoid congestion in the figure. Our calculations confirm the existence of a sharp resonance on the $^2\Pi$ scattering symmetry centred at around 1.2 eV as reported by Lynch *et al* (1979). As pointed out by Lynch *et al* (1979), the resonance is of d-wave ($l = 2$) nature. Nevertheless, our calculation has also revealed important p-wave ($l = 1$) contributions at this energy region. The measured data of Sohn *et al* (1987) do not show evidence of such a resonance structure. This is probably due to the fact that their measurements were carried out at a few sparsely distributed incident energies. On the other hand, this resonance is clearly seen in the measured TCS of Szmytkowski *et al* (1984) and Sueoka *et al* (1999), as shown in figure 1(*b*). The resonance features near this energy region are also seen in the electron-impact dissociative attachment experiments (Abouaf *et al* 1994, Iga and Srivastava 1995).

Quantitatively, our calculated ICS are also in very good agreement with the theoretical results of Lynch *et al* (1979). When compared with experiments, our ICS are in good agreement with the present measured data in the 100–600 eV range and with the data reported by Sohn *et al* (1987) except in the resonance region. On the other hand, the ICS for elastic e^-–OCS scattering reported by Sueoka *et al* (1999) lie systematically below. Further, our calculated TCS are in good agreement with the measured data in the entire energy range covered herein, except in the resonance region where our calculation overestimates the TCS. Also, the calculated resonance width is narrower than that observed experimentally. These discrepancies probably arise from the effects of nuclear motion, not included in the present calculation. On the other hand, our calculation strongly overestimates ICS and TCS at incident energies below 1 eV.

Table 1. Present measured DCS and ICS (in 10^{-16} cm^2) for elastic e$^-$–OCS scattering.

Angle	E_0 (eV)						
(deg)	100	150	200	300	400	500	600
10	19.75	12.36	9.98	8.10	6.20	4.62	4.08
15	8.33	7.19	4.37	2.66	2.46	2.34	2.07
20	3.37	3.48	2.09	1.41	1.08	1.12	0.988
25	1.77	1.93	0.971	0.737	0.717	0.702	0.629
30	0.994	1.06	0.571	0.527	0.486	0.478	0.383
35	0.592	0.673	0.440	0.366	0.327	0.355	0.249
40	0.391	0.521	0.347	0.250	0.233	0.207	0.157
45	0.302	0.423	0.270	0.182	0.167	0.134	0.112
50	0.255	0.351	0.219	0.137	0.115	0.103	0.084
55	0.220	0.290	0.178	0.101	0.093	0.078	0.070
60	0.190	0.246	0.148	0.077	0.073	0.063	0.056
65	0.174	0.214	0.123	0.061	0.064	0.051	0.044
70	0.158	0.180	0.106	0.052	0.055	0.042	0.037
75	0.147	0.152	0.094	0.047	0.047	0.036	0.032
80	0.136	0.132	0.080	0.039	0.041	0.029	0.027
85	0.128	0.110	0.073	0.034	0.037	0.028	0.023
90	0.112	0.100	0.067	0.030	0.035	0.027	0.020
95	0.100	0.089	0.059	0.027	0.033	0.026	0.019
100	0.085	0.079	0.058	0.025	0.031	0.025	0.018
105	0.075	0.069	0.058	0.027	0.031	0.024	0.018
110	0.070	0.067	0.060	0.027	0.032	0.025	0.019
115	0.068	0.076	0.063	0.029	0.035	0.025	0.020
120	0.073	0.090	0.071	0.035	0.037	0.025	0.020
125	0.083	0.112	0.078	0.040	0.040	0.026	0.021
ICS	8.171	6.639	5.011	3.644	3.031	2.469	2.119

We cannot attribute this discrepancy convincingly to a specific physical origin. At such low incident energies, probably the electronic correlation effects of the target can play important roles in the dynamics of electron–molecule collisions. Unfortunately, the inclusion of target correlation effects to electron–molecule scattering calculations is still an open problem.

In figures 2–5 we show our calculated DCS for elastic electron–OCS scattering in the 1.15–100 eV energy range along with the available experimental data of Sohn *et al* (1987) and Tanaka (2000). At 100 eV, our present measured data are shown as well for comparison. The data reported by Sohn *et al* (1987) are vibrationally resolved. Therefore the comparison is made with the sum of their DCS for vibrationally elastic collisions and those for the $v = 0 \rightarrow v' = 1$ vibrational excitations, including both the stretching and bending modes. DCS for excitation to higher vibrational levels are small and are then neglected. In general, our calculated DCS are in good qualitative agreement with the measured data in this energy range, except for 1.15 eV. At that energy, the minimum seen in the experimental data located approximately at 100° is shifted to near 60°. Also for that energy, the quantitative agreement between the calculated and measured data is poor. The reason for this discrepancy is probably the same as those seen for ICS and TCS in the low-energy range. At higher incident energies, the agreement between theory and experiment is much better. The best agreement between theory and experiment lies in the 5–100 eV range. However, even at an incident energy as low as 2 eV, a good agreement with experimental data, both qualitatively and quantitatively, is seen.

Above 100 eV, there are no other experimental results reported in the literature. Therefore, in figures 6 and 7 we compare our calculated DCS in the 150–600 eV range with the present measured data. In the 150–300 eV range, the agreement between the calculated and measured DCS is good. At higher energies, although our calculation underestimates the DCS at large scattering angles, the agreement with the measured data is very good in the small and intermediate scattering angles, which is very encouraging.

For the sake of completeness, in table 1 we show our measured cross sections.

In summary, we present a joint theoretical and experimental study on elastic electron scattering by OCS molecules in the low- and intermediate-energy ranges. A complex optical potential is used to represent the collisional dynamics. Our calculation confirms the existence of a shape resonance of π symmetry centred at around 1.2 eV, which is in good agreement with the experimental observations. Our calculated DCS are also in general good agreement with the present measured data and experimental results available in the literature. The discrepancy between the calculated and experimental cross sections seen at low incident energies is attributed to the neglect of the electronic correlation effects of the target. Accounting for the correlation effects of the target into electron–molecule scattering still constitutes a challenge to theorists and would be a subject for our future investigation.

Acknowledgments

This work is partially supported by the Brazilian agencies FINEP-PADCT, CNPq and FAPESP. We would also like to thank Professor H Tanaka for sending us the experimental data prior to publication.

References

Abouaf R, Pommier J, Cvejanovic S and Saubaméa B 1994 *Chem. Phys.* **188** 339
Alle D T, Gulley R J, Buckman S J and Brunger M J 1992 *J. Phys. B: At. Mol. Opt. Phys.* **25** 1533
Brinkman R T and Trajmar S 1981 *J. Phys. E: Sci. Instrum.* **14** 245
Brunger M J, Buckman S J, Newman D J and Alle D T 1991 *J. Phys. B: At. Mol. Opt. Phys.* **24** 1435
Buckman S J, Gulley R J, Moghbelalhossein M and Bennett S J 1993 *Meas. Sci. Technol.* **4** 1143
Bündgen P, Grein F and Thakkar A J 1995 *J. Mol. Struct. (Theochem)* **334** 7
Dababneh M S, Hsieh Y-F, Kauppila W E, Kwan C K and Stein T S 1985 *Proc. 14th Int. Conf. on Physics of Electronic and Atomic Collisions (Palo Alto, CA)* Abstracts of Contributed Papers p 230
Dunning T H 1971 *J. Chem. Phys.* **55** 716
Fliflet A W and McKoy V 1980 *Phys. Rev.* A **21** 1863
Hehere W J, Radom L, Schleyer P V R and Pople J A 1986 *Ab initio Molecular Orbital Theory* (New York: Wiley) p 174
Hirschfelder J O, Curtis C F and Bird R B 1954 *Molecular Theory of Gases and Liquids* (New York: Wiley)
Huzinaga S 1965 *J. Chem. Phys.* **42** 1293
Iga I, Homem M G P, Mazon K T and Lee M-T 1999 *J. Phys. B: At. Mol. Opt. Phys.* **32** 4373
Iga I, Lee M-T, Homem M G P, Machado L E and Brescansin L M 2000 *Phys. Rev.* A **61** 22 708–1
Iga I and Srivastava S K 1995 *J. Mol. Struct. (Theochem.)* **335** 31
Jansen R H J, de Heer F J, Luyken H J, van Wingerden B and Blaauw H J 1976 *J. Phys. B: At. Mol. Phys.* **9** 185
Khakoo M A, Jayawera T, Wang S and Trajmar S 1993 *J. Phys. B: At. Mol. Opt. Phys.* **26** 4845
Khakoo M A and Trajmar S 1986 *Phys. Rev.* A **34** 138
Lee M-T, Brescansin L M and Lima M A P 1990a *J. Phys. B: At. Mol. Opt. Phys.* **23** 3859
Lee M-T, Brescansin L M, Lima M A P, Machado L E and Leal E P 1990b *J. Phys. B: At. Mol. Opt. Phys.* **23** 4331
Lee M-T, Fujimoto M M, Michelin S E, Machado L E and Brescansin L M 1992 *J. Phys. B: At. Mol. Opt. Phys.* **25** L505
Lee M-T and Iga I 1999 *J. Phys. B: At. Mol. Opt. Phys.* **32** 453
Lee M-T and McKoy V 1983 *Phys. Rev.* A **28** 697
Lee M-T, Michelin S E, Kroin T and Veitenheimer E 1999 *J. Phys. B: At. Mol. Opt. Phys.* **32** 3043

Lide D V (ed) 1993 *Handbook of Chemistry and Physics* (Boca Raton, FL: CRC Press) p 73
Lucchese R R, Raseev G and McKoy V 1982 *Phys. Rev.* A **25** 2572
Lynch M G, Dill D, Siegel J and Dehmer J L 1979 *J. Chem. Phys.* **71** 4249
Michelin S E, Kroin T and Lee M-T 1996 *J. Phys. B: At. Mol. Opt. Phys.* **29** 2115
Nickel J C, Zetner P W, Shen G and Trajmar S 1989 *J. Phys. E: Sci. Instrum.* **22** 730
Olander D R and Kruger V 1970 *J. Appl. Phys.* **41** 2769
Roth A 1982 *Vacuum Technology* (Amsterdam: North-Holland)
Padial N T and Norcross D W 1984 *Phys. Rev.* A **29** 1742
Sohn W, Kochem K-H, Sheuerleim K-M, Jung K and Ehrhardt H 1987 *J. Phys. B: At. Mol. Phys.* **20** 3217
Srivastava S K, Chutjian A and Trajmar S 1975 *J. Chem. Phys.* **63** 2659
Staszewska G, Schwenke D W and Truhlar D G 1984 *Phys. Rev.* A **29** 3078
Sueoka O, Hamada A, Kimura M, Tanaka H and Kitajima M 1999 *J. Chem. Phys.* **111** 245
Szmytkowski 1987 *J. Phys. B: At. Mol. Phys.* **20** 6613
Szmytkowski C, Karwasz G and Maciag K 1984 *Chem. Phys. Lett.* **107** 481
Szmytkowski C, Maciag K, Karwasz G and Filipovic D 1989 *J. Phys. B: At. Mol. Opt. Phys.* **22** 525
Tanaka H 2000 at press
Tanaka H, Ishikawa T, Masai T, Sagara T, Boesten L, Takekawa M, Itikawa Y and Kimura M 1998 *Phys. Rev.* A **57** 1798
Tronc M, King G C and Read F H 1979 *J. Phys. B: At. Mol. Phys.* **12** 137
Zecca A, Nogueira J C, Karwasz g P and Brusa R S 1995 *J. Phys. B: At. Mol. Opt. Phys.* **28** 477
Ziesel K F, Miletić M and Veljković M 1980 *Bull. Soc. Chim. Belgrad.* **45** 23